Lumped Parameter Thermal Network Identification for Transient System Response Prediction of Automotive Components

Maximilian Kehe, Wolfram Enke, Hermann Rottengruber

EG-623
BMW AG
Knorrstraße 147, 80788 München

maximilian.kehe@bmw.de
wolfram.enke@bmw.de
hermann.rottengruber@ovgu.de

Abstract: This work presents a systematic approach to identify the thermal behavior of arbitrary automotive component systems. The proposed methodology leverages experimental temperature data and prior knowledge from Computational Fluid Dynamics (CFD) simulations to achieve a consistent system identification. The key aspects of the approach include thermal behavior identification through minimizing the least-squared error between the predicted thermal lumped parameter model and the experimentally measured temperature data, ensuring a robust and accurate representation of the system's thermal characteristics. The identified system model is then utilized to generate transient system responses for defined use-cases, enabling a comprehensive understanding of the thermal behavior under various operating conditions. The identification algorithm is based on the least-square programming algorithm from SciPy, providing a robust and efficient computational framework. Ensuring the reliability and durability of automotive components is crucial, as they must withstand the wide range of temperatures encountered during operation. To this end, the temperature-critical components are experimentally tested and simulated using CFD. The proposed methodology offers the capability to understand thermal interactions in experimental data and to generate transient responses based on stationary CFD simulations. Additionally, this work lays the groundwork for predicting temperatures in future vehicles with physics-informed neural networks. The method is tested with experimental temperature data and a numerical model of the component space of one control unit in the A-pillar of BMW's current 7 Series.

Contribution: 2025 FKFS Conference on Vehicle Aerodynamics and Thermal Management
15 – 16 October 2025 | Leinfelden-Echterdingen

1 Introduction

The thermal operating safety (TOS) of automotive vehicles is becoming increasingly challenging due to the rising complexity of the products. TOS focuses on ensuring that all components can withstand the thermal loads they encounter throughout their lifespan [FrER23]. Historically, the primary emphasis of TOS has been on components associated with or near combustion engines, such as engine rubber mounts [FrRE24]. The combination of extreme weather conditions, limited component space, cost pressures, and rising computational demands has added additional components to the scope of TOS, such as electronic control units (ECUs). This has compelled the automotive industry to take the lead in investing in thermal management for electronic devices [DhKA23].

The primary objective of TOS is to evaluate all critical components and implement cooling measures when necessary. To assess TOS, two main data sources are utilized: experimental testing and simulation. At BMW the experimental testing is conducted at the environmental test center in Munich [Bmwa25]. While experimental testing provides accurate and transient temperature data, it is both time-consuming and costly. It requires expensive prototypes and wind tunnel capacity, and testing must continue until a stationary state is reached. On the other hand, the capabilities of computational fluid dynamics (CFD) simulations have significantly improved in recent years, allowing for the assessment of TOS issues, such as heat transfer in exhaust systems [AhRF22, Enri15]. CFD simulations enable the evaluation of a wide range of boundary conditions and various TOS measures in a relatively short time frame. To determine the reliability of a component, it is essential to consider its cumulative thermal load over its lifetime, as components can experience fatigue not only from exceeding certain temperature thresholds [Elle17]. Consequently, TOS employs transient use cases to capture the complete temperature bandwidth. This approach has led to numerous publications on transient CFD simulations [Disc16, Gheb13]. However, for the TOS use-cases at BMW the experience shows, that transient CFD simulations are 4 to 10 times more expensive than stationary simulations.

To leverage the strengths of both methods, this paper proposes a combined approach that integrates the transient behavior derived from experimental data with the rapid calculations enabled by CFD simulations. Specifically, a zero-dimensional physical representation of thermal systems, known as the Lumped Parameter Thermal Network (LPTN), is utilized [MeRT91]. The parameters of the LPTN can be estimated with a minimization algorithm, allowing for the calculation of transient behavior [KeRE25]. In this study, the methodology is demonstrated using an E/E component from the G70 BMW, referred to as ‘IPBasis.’ The paper begins by explaining the mathematical modeling of the LPTN for this component space. Next, the transient behavior, represented by heat capacities, is fitted using multiple experimental data sets. The heat transfer parameters are then derived from the corresponding stationary CFD simulations. Finally, the combined LPTN is constructed using the fitted parameters, and the transient temperature curve is generated.

2 Mathematical Framework

To demonstrate the combined approach, first, the theory of the lumped parameter thermal network must be shortly introduced. A more detailed explanation is provided in [KeRE25]. First, the LPTN is introduced for the component space of the IPBasis, and the fundamental equations are derived. Secondly, the state-space approach to calculate the transient response of the LPTN is explained. Lastly, the minimization algorithm to derive the parameters of the LPTN from given data is tackled.

2.1 Modeling of Lumped Parameter Thermal Networks (LPTN)

Lumped parameter thermal networks are based on an energy formulation of lumped masses. Hence, this approach assumes that within these masses a homogeneous temperature is present. The energy approach results in a 0D formulation as there is no dependency on place. Two further simplifications are made in the current implementation of the LPTN. On the one hand, it is based on constants for heat capacities and heat transfer coefficients. Hence, temperature dependent effects like change of convection are averaged. On the other hand, radiation effects are not included, which simplifies the equations to a linear system.

In figure 1 the LPTN for the component space of the IPBasis is displayed. It consists of two bodies, the chassis and the IPBasis. The two bodies are connected by conduction. The chassis has a convection term to the outside temperature T_{ext}. The IPBasis is connected to the interior by convection which has the temperature T_{int}. The system is heated by the waste heat of the IPBasis $\dot{Q}_2^{\text{waste}}$.

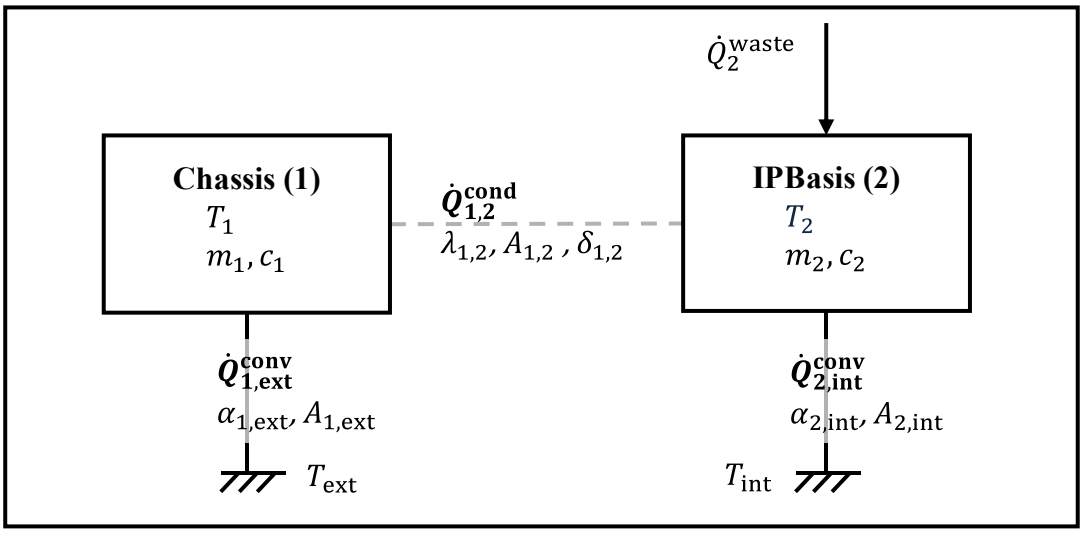

Figure 1: Lumped Parameter Thermal Network.

The lumped parameter thermal network can now be mathematically formulated by building the energy equilibrium of each body. The resulting two equations describing the time-dependent behavior of the system are displayed in equation 2.1.

$$
\begin{aligned}
m_1 c_1 \dot{T}_1 &= \frac{\lambda_{1,2} A_{1,2}}{\delta_{1,2}} (T_2 - T_1) + \alpha_{1,\mathrm{ext}} A_{1,\mathrm{ext}} (T_{\mathrm{ext}} - T_1) \\
m_2 c_2 \dot{T}_2 &= \frac{\lambda_{1,2} A_{1,2}}{\delta_{1,2}} (T_1 - T_2) + \alpha_{2,\mathrm{int}} A_{2,\mathrm{int}} (T_{\mathrm{ext}} - T_2) + \dot{Q}_2^{\mathrm{waste}}
\end{aligned}
\tag{2.1}
$$

2.2 Calculate Time-Response of LPTN

To calculate the time response of the LPTN, the state-space representation is leveraged. The general formulation in matrix form is displayed in equation 2.2.

$$
\dot{\boldsymbol{T}} = \boldsymbol{A}\boldsymbol{T} + \boldsymbol{B} \tag{2.2}
$$

In the next step, the energy equations from 2.1 can be reformulated in the A and B matrices. The resulting matrices are shown in the following equation:

$$
\begin{bmatrix} \dot{T}_1 \\ \dot{T}_2 \end{bmatrix} = \begin{bmatrix} -\frac{\lambda_{1,2} A_{1,2}}{m_1 c_1 \delta_{1,2}} - \frac{\alpha_{1,\mathrm{ext}} A_{1,\mathrm{ext}}}{m_1 c_1} & \frac{\lambda_{1,2} A_{1,2}}{m_1 c_1 \delta_{1,2}} \\ \frac{\lambda_{1,2} A_{1,2}}{m_2 c_2 \delta_{1,2}} & -\frac{\lambda_{1,2} A_{1,2}}{m_2 c_2 \delta_{1,2}} - \frac{\alpha_{2,\mathrm{int}} A_{2,\mathrm{int}}}{m_2 c_2} \end{bmatrix} \begin{bmatrix} T_1 \\ T_2 \end{bmatrix} + \begin{bmatrix} \frac{\alpha_{1,\mathrm{ext}} A_{1,\mathrm{ext}}}{m_1 c_1} T_0 \\ \frac{1}{m_2 c_2} \dot{Q}_2^{\mathrm{waste}} + \frac{\alpha_{2,\mathrm{int}} A_{2,\mathrm{int}}}{m_2 c_2} T_{\mathrm{int}} \end{bmatrix} \tag{2.3}
$$

Finally, the time response of the LPTN in form of the temperatures $T(t)$ can be calculated by using the Runge-Kutta method of fourth order. The method is a standard solver for ordinary differential equations. Next to the matrices, the method needs initial temperatures $\boldsymbol{T}_0$, a simulation time step $\mathrm{d}t$, and the time interval $[t_0, t_{\mathrm{end}}]$. The calculation can be written as follows:

$$
\boldsymbol{T}(t) = \mathrm{RK4}(\boldsymbol{A}, \boldsymbol{B}, \boldsymbol{T}_0, \mathrm{d}t, [t_0, t_{\mathrm{end}}]) \tag{2.4}
$$

2.3 Calculate LPTN Parameters from Temperature Data

The idea is to find the parameters of the LPTN from only the temperature information. There are two concerns with this approach. First, there are unlimited combinations of the matrix A and B and therefore of the parameters that can show the same behavior as the data. Hence, this is considered an ill-posed problem. To tackle this issue, the parameters are fitted by a minimization algorithm to find the best fit. Secondly, multiplied values like $m_2 c_2$ cannot be distinguished, hence they need a surrogate parameter. These parameters are called identifiable, as they satisfy the necessary condition to be distinguishable. The list of identifiable parameters is provided in table 1.

Definition	Identifiable Parameter	Replaced Parameters	Unit
Heat Capacity	C^m	mc_p	J/K
Convection Term	C^α	αA	W/K
Conduction Term	C^λ	$\lambda A \,/\, \delta$	W/K
Boundary Heat Flux	$\dot{Q}$	$\dot{Q}$	W

Table 1: Table of the identifiable parameters.

The set of identifiable parameters is denoted with $\boldsymbol{\vartheta}$ and can be seen in the following equation:

$$\boldsymbol{\vartheta} = [\boldsymbol{C}_m, \boldsymbol{C}_\alpha, \boldsymbol{C}_\lambda, \dot{\boldsymbol{Q}}\,] \tag{2.5}$$

With the identifiable parameters the LPTN model is simplified. This is exemplary shown in equation 2.6 for the state-space representation.

$$\begin{bmatrix}\dot{T}_1\\ \dot{T}_2\end{bmatrix} = \begin{bmatrix} -\frac{C^\lambda_{1,2}}{C^m_1} - \frac{C^\alpha_{1,\mathrm{ext}}}{C^m_1} & \frac{C^\lambda_{1,2}}{C^m_1} \\ \frac{C^\lambda_{1,2}}{C^m_2} & -\frac{C^\lambda_{1,2}}{C^m_2} - \frac{C^\alpha_{2,\mathrm{int}}}{C^m_2} \end{bmatrix} \begin{bmatrix}T_1\\ T_2\end{bmatrix} + \begin{bmatrix} \frac{C^\alpha_{1,\mathrm{ext}}}{C^m_1} T_{ext} \\ \frac{1}{C^m_2}\dot{Q}_2^{\mathrm{waste}} + \frac{C^\alpha_{2,\mathrm{int}}}{C^m_2} T_{\mathrm{int}} \end{bmatrix} \tag{2.6}$$

Now, the minimization algorithm can be applied. The goal of the minimization is to find the parameter set $\boldsymbol{\vartheta}^{\min}$ that minimizes the error between the data $\boldsymbol{T}^{\mathrm{Data}}$ and the calculated system response of the LPTN $\boldsymbol{T}^{\min}$. The minimization term $\boldsymbol{\varepsilon}$ is calculated by the mean squared error:

$$\boldsymbol{\varepsilon} = \left(\boldsymbol{T}^{\mathrm{Data}} - \boldsymbol{T}^{\min}\right)^2$$
$$\text{With: } \boldsymbol{T}^{\min} = \mathrm{RK4}\left(\boldsymbol{A}(\boldsymbol{\vartheta}^{\min}), \boldsymbol{B}(\boldsymbol{\vartheta}^{\min}), \boldsymbol{T}_0^{\mathrm{Data}}, \mathrm{d}t, [t_0, t_{\mathrm{end}}]\right) \tag{2.6}$$

The calculated parameters provide a combination that fits the provided data the best. However, these parameters are not necessarily the correct physical parameters of the system. In the original paper it was proposed to fit over multiple files simultaneously to get a global and uniform estimation. This way, the heat coefficients can be compared between the files and the estimated heat capacities are representative of the system response as they describe multiple files. This approach is conducted in the next chapter for the experimental data.

3 Experimental Data

The goal of this chapter is to retrieve the global heat capacities ($C_1^{m,ED}, C_2^{m,ED}$) from the experimental data (ED). Figure 2 displays an overview of the LPTN that is minimized for this purpose. Every dataset contains the experimental temperatures (T_1^{ED}, T_2^{ED}) and the boundary conditions ($\dot{Q}_2^{\mathrm{waste}}, T_{\mathrm{ext}}, T_{\mathrm{int}}$). The global parameters (C_1^m, C_2^m) are used for all files. The local parameters ($C_{1,2}^{\lambda}, C_{1,\mathrm{ext}}^{\alpha}, C_{2,\mathrm{int}}^{\alpha}$) are fitted for each file. The hypothesis is that the masses and materials remain the same, but the heat transfer coefficients vary from file to file due to different boundary conditions.

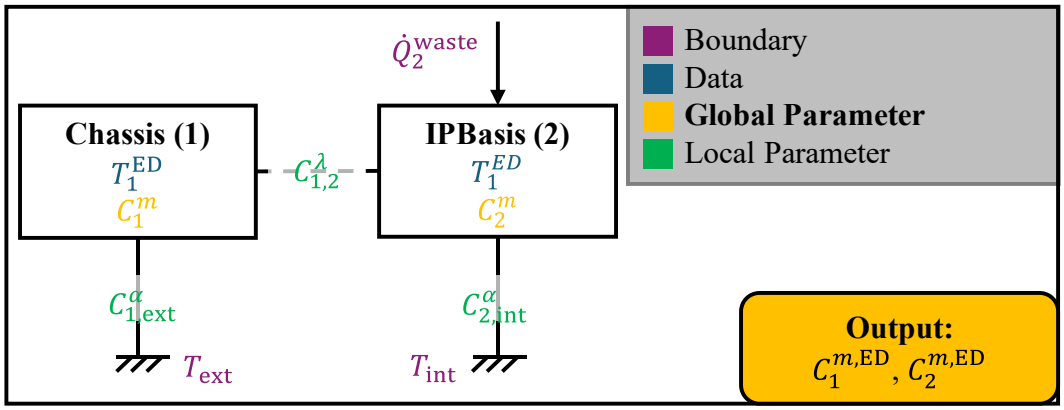

Figure 2: LPTN System to identify the global parameters in form of the heat capacities.

The data used for this approach is gained from windtunnel testing of the BMW G70 model. An overview of the test setup can be found in figure 3.

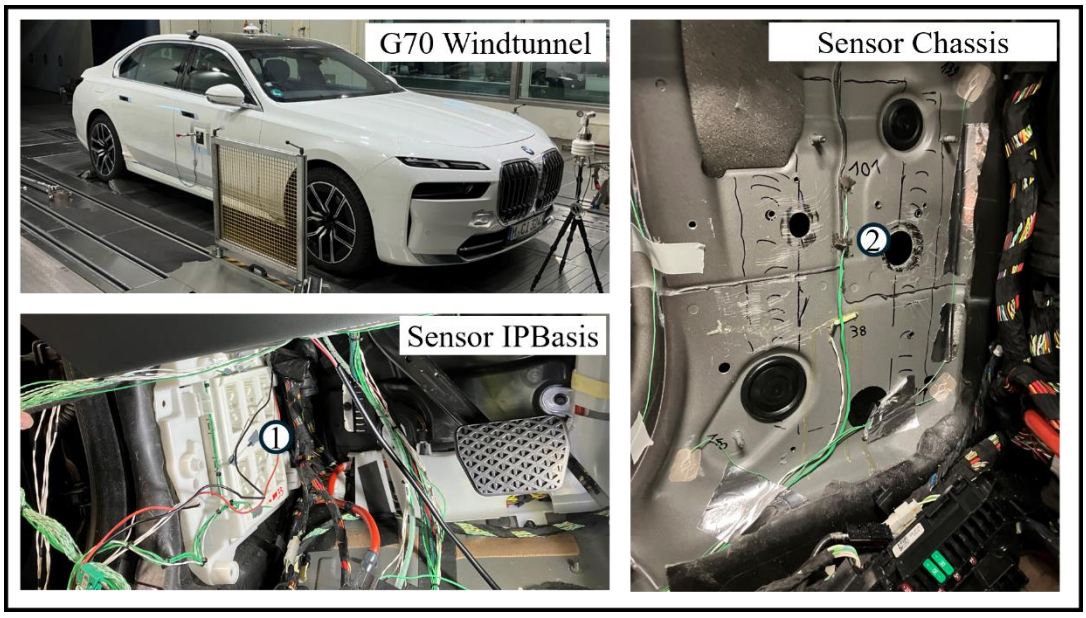

Figure 3: Measurement of the experimental data. The upper left corner is an exemplary picture of the G70 in the environmental testing center. In the lower left corner, the sensor placement at the IPBasis is shown. On the right the sensor placement at the chassis is displayed.

In the upper left of figure 3 an exemplary picture of a G70 in the environmental test center is displayed. The sensor placements inside of the IPBasis and at the surface of the chassis are displayed in the other two graphics.

In this setup multiply tests were conducted like Stop&Go, Soakbox heating, and Vmax. To get the most homogeneous data for the minimization, the initial heating phase during constant boundary conditions were segmented from the rest of the test periods. The representative LPTN for each file is build and the global heat capacities as well as the local heat transfer coefficients is found by fitting to the experimental data ($\boldsymbol{T}_1^{\mathrm{ED}}$, $\boldsymbol{T}_2^{\mathrm{ED}}$). The time responses of the fitted LPTN after the minimization ($\boldsymbol{T}_1^{\mathrm{min}}$, $\boldsymbol{T}_2^{\mathrm{min}}$) are shown in figure 4. Three measurements are displayed exemplarily.

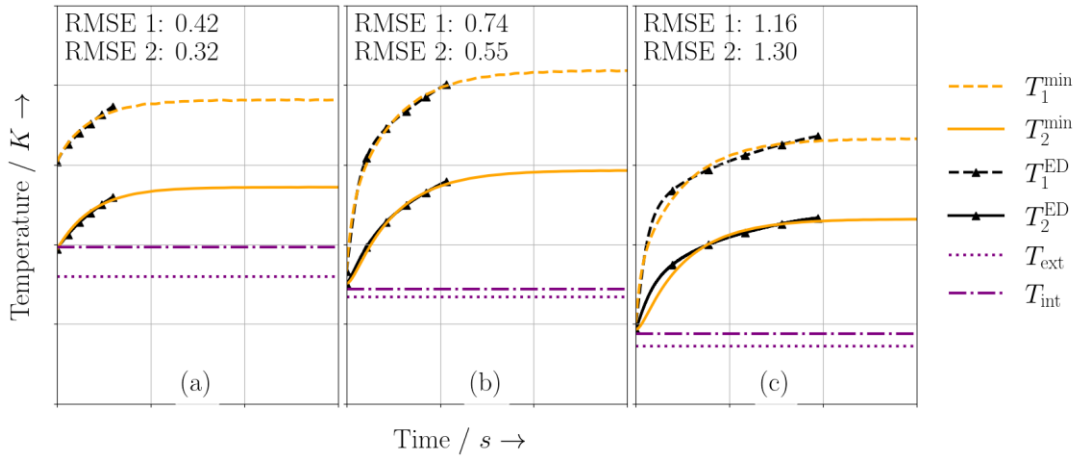

Figure 4: This graphic shows the global parameter estimation of three experimental measurements. Subfigure (a), (b), and (c) each show a different experimental setup with varying boundary conditions.

The fitting was able to capture the heating behavior of all files to an average root mean squared error (RMSE) of 0.91K. The RMSE of the IPBasis is slightly higher with 1.03°C compared to the chassis with 0.79°C, but the IPBasis is also generally significantly warmer. The results indicate that the global heat capacities $C_1^{m,\mathrm{ED}}$ and $C_2^{m,\mathrm{ED}}$ found are a good representative of the overall behavior of the system.

4 CFD Data

In the next step the heat transfer coefficients ($C_{1,2}^{\lambda,\mathrm{CFD}}, C_{1,\mathrm{ext}}^{\alpha,\mathrm{CFD}}, C_{2,\mathrm{int}}^{\alpha,\mathrm{CFD}}$) are found from the CFD-Simulation results. The CFD simulation is stationary, hence the temperatures ($T_1^{\mathrm{CFD,stat}}$, $T_2^{\mathrm{CFD,stat}}$) are of scalar nature. The CFD simulation can calculate the temperature results for arbitrary boundary conditions ($\dot{Q}_2^{\mathrm{waste}}, T_{\mathrm{ext}}, T_{\mathrm{int}}$). As only stationary information is available, the heat capacities ($C_1^{m,\mathrm{ED}}, C_2^{m,\mathrm{ED}}$) are not relevant for the calculation of the heat transfer coefficients. The overview of the LPTN for the fitting of the CFD parameters is provided in figure 5.

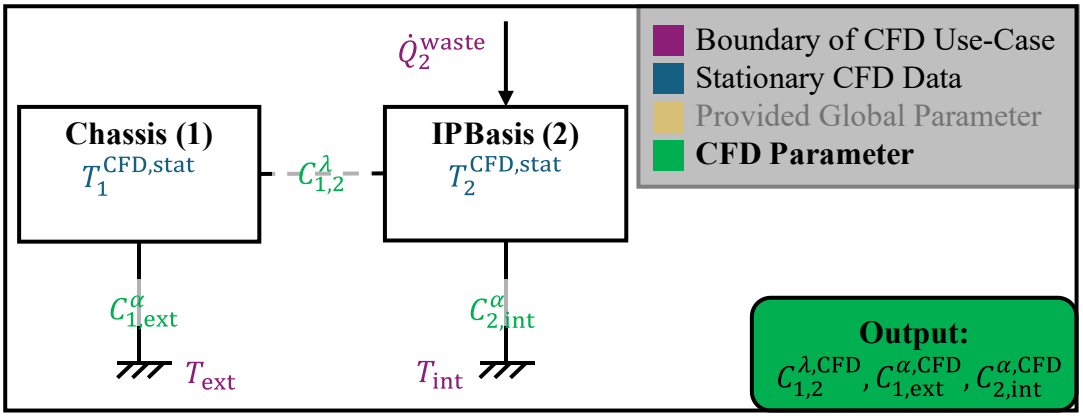

Figure 5: LPTN System to identify the conduction and convection parameter from the stationary CFD-Simulation.

In figure 6 an overview of the CFD simulation is provided. The boundary conditions are imprinted on the model by setting the external temperature at the bottom of the cassis and by setting a Dirichlet boundary condition in the air space of the IPBasis. The sensors are placed in the same locations as the experimental data, the IPBasis sensor is in the inside of the ECU and the Chassis temperature is taken at the surface of the chassis.

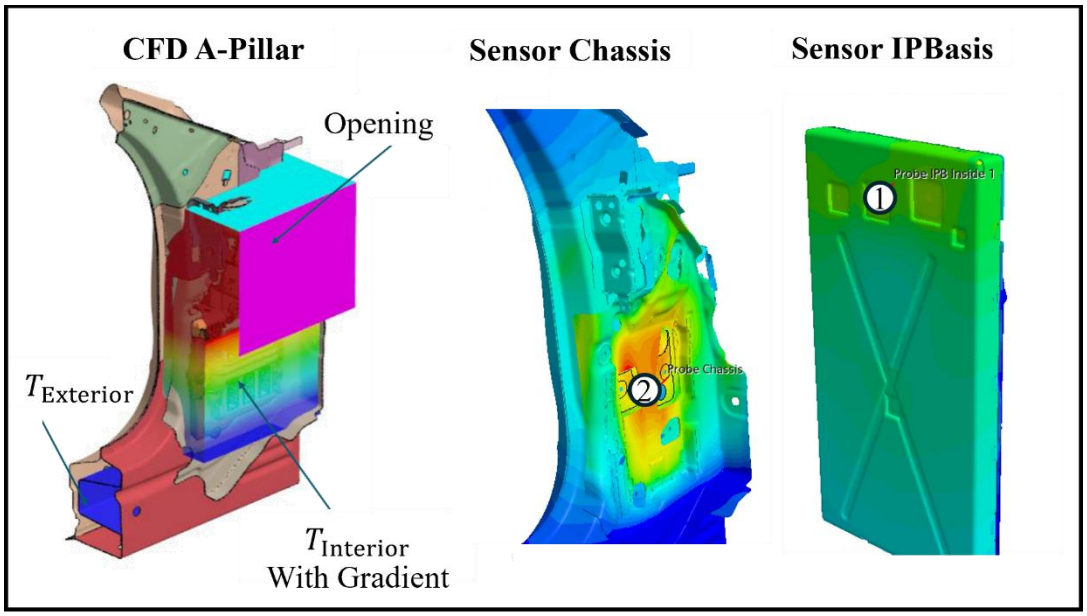

Figure 6: Overview of the CFD-Simulation.

As the temperature of the CFD is stationary, the state-space representation is simplified, and the heat capacities can be neglected. This is shown in equation 4.1.

$$\begin{bmatrix}0\\0\end{bmatrix} = \begin{bmatrix} -C_{1,2}^{\lambda,\text{CFD}} - C_{1,\text{ext}}^{\alpha,\text{CFD}} & C_{1,2}^{\lambda,\text{CFD}} \\ C_{1,2}^{\lambda,\text{CFD}} & -C_{1,2}^{\lambda,\text{CFD}} - C_{2,\text{int}}^{\alpha,\text{CFD}} \end{bmatrix} \begin{bmatrix} T_1^{\text{CFD,stat}} \\ T_2^{\text{CFD,stat}} \end{bmatrix} + \begin{bmatrix} C_{1,\text{ext}}^{\alpha,\text{CFD}} T_{\text{ext}} \\ \dot{Q}_2^{\text{waste}} + C_{2,\text{int}}^{\alpha,\text{CFD}} T_{\text{int}} \end{bmatrix} \tag{4.1}$$

This system has three unknowns ($C_{1,2}^{\lambda,\mathrm{CFD}}, C_{1,\mathrm{ext}}^{\alpha,\mathrm{CFD}}, C_{2,\mathrm{int}}^{\alpha,\mathrm{CFD}}$), but only two equations, hence it is underdetermined. The minimization algorithm is capable of still finding a set of parameters that will result in the correct stationary temperatures. However, to find a unique solution, an additional condition is necessary. Fortunately, it is comparably easy to retract additional information from a CFD simulation, like the heat flux over a defined area. Here, the heat flux to the exterior $\dot{Q}_{\mathrm{ext}}^{\mathrm{CFD}}$ is used as an additional condition. With this information, the system is determined. In this paper we reuse the minimization algorithm to calculate the parameters. The adjusted loss function can be seen in equation 4.2.

$$\boldsymbol{\varepsilon} = \left(T_1^{\mathrm{CFD,stat}} - \boldsymbol{T}^{\mathrm{min}}\right)^{\mathbf{2}} + \left(\dot{Q}_{\mathrm{ext}}^{\mathrm{CFD}} - \dot{Q}_{\mathrm{ext}}^{\mathrm{min}}\right)^{\mathbf{2}}$$

$$\text{With: } \boldsymbol{T}^{\mathrm{min}} = \boldsymbol{A}(\boldsymbol{\vartheta}^{\mathrm{min}}) \backslash \boldsymbol{B}(\boldsymbol{\vartheta}^{\mathrm{min}}) \tag{4.2}$$

$$\text{With: } \dot{Q}_{\mathrm{ext}}^{\mathrm{min}} = C_{1,\mathrm{ext}}^{\alpha,\mathrm{CFD}}(T_{\mathrm{ext}} - T_1^{\mathrm{min}})$$

As this is a determined problem, the calculated parameters ($C_{1,2}^{\lambda,\mathrm{CFD}}, C_{1,\mathrm{ext}}^{\alpha,\mathrm{CFD}}, C_{2,\mathrm{int}}^{\alpha,\mathrm{CFD}}$) are the correct description of the CFD simulation for the specific use-case. One issue is the fact that the heat transfer coefficients are found from the stationary point, here the hottest point of the use-case. Hence, the fitted parameters might overestimate the actual parameters over the complete heating period. This concern is especially relevant for the convection parameters, as they are usually temperature dependent. One solution for this problem could be to include a time-dependent nonlinearity in the convection parameters, for example linear interpolation from the initial state to the stationary state. However, this is not further investigated in this work. For the present use-case for the IPBasis the overestimation is assumed to be acceptable, as the overall temperature delta is not over 100K.

5 Combined LPTN

5.1 Proof of Concept

In a first step, the overall concept needs to be demonstrated. For this, a pragmatical approach is chosen which is displayed in figure 7. An artificial LPTN is designed, and for four use-cases artificial data (T_1^{AD}, T_2^{AD}) is generated. The heat capacities are found by minimizing three use-cases, one is shown exemplary in the (a). The fourth use-case is the ground truth (T_1^{Truth}, T_2^{Truth}). The heat transfer coefficients are calculated from the stationary data and one heat flux condition. This is displayed in (b). The parameters are then combined in a LPTN and simulated. The resulting temperatures (T_1^{combined}, T_2^{combined}) can be seen in (c). The figure shows that the combined temperatures exactly match the ground truth data. This proves that the concept to fit the masses from different use-cases and calculate the transient response of stationary data is viable.

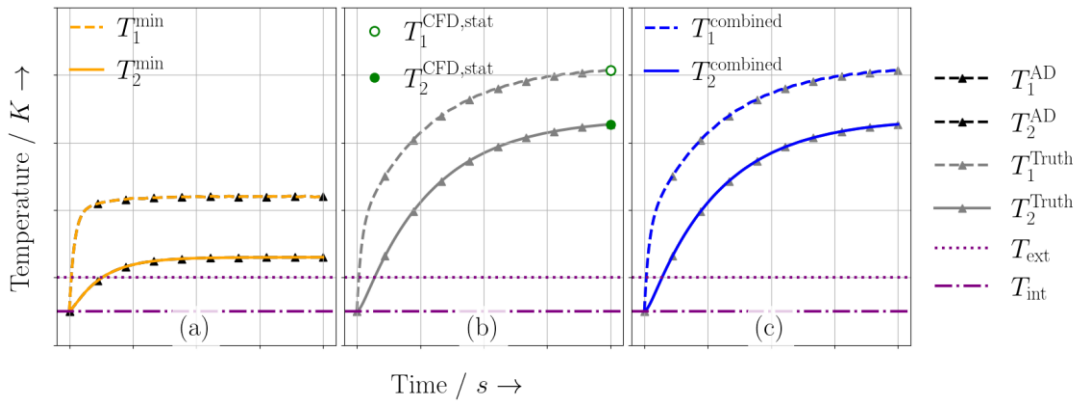

Figure 7: Proof of Concept for the correct calculation of the transient curves when the parameters are calculated from the stationary point. Subfigure (a) is the heat capacity minimization, (b) is the stationary CFD data, and (c) is the calculated LPTN response from the combined parameters.

5.2 Calculating the transient response for the IPBasis

At this point, all the necessary parameters to calculate the transient response for the CFD use-case are gained. The effective heat capacities ($C_1^{m,\text{ED}}, C_2^{m,\text{ED}}$) from the experimental data are fitted. The use-case specific heat transfer coefficients ($C_{1,2}^{\lambda,\text{CFD}}, C_{1,\text{ext}}^{\alpha,\text{CFD}}, C_{2,\text{int}}^{\alpha,\text{CFD}}$) from the CFD simulation are found for the LPTN. The goal is to calculate the transient temperatures (T_1^{Combined}, T_2^{Combined}). This can be achieved by building the LPTN from the known parameters. The LPTN system is displayed in figure 8.

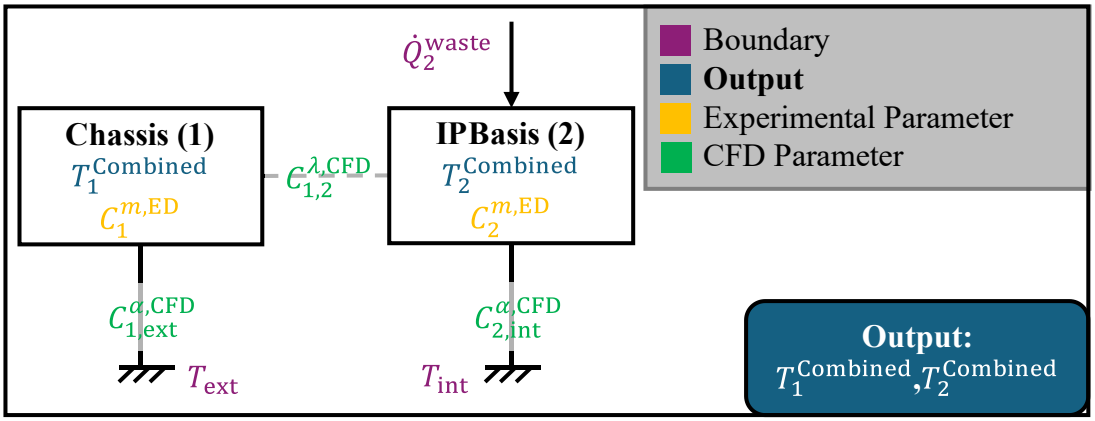

Figure 8: LPTN System Overview for combining the parameters from experiment and CFD-Simulation.

With this LPTN, the RK4 method can calculate the time response. The result is shown in figure 9. This calculation is the result this work was aiming for. The assessment of this result is not straightforward, as this combination of experimental and simulation data has created a new kind of information, which has no ground truth. This result is accurate if the masses and the heat capacities are identified correctly. The assessment of the fitting accuracy is not scope of this work.

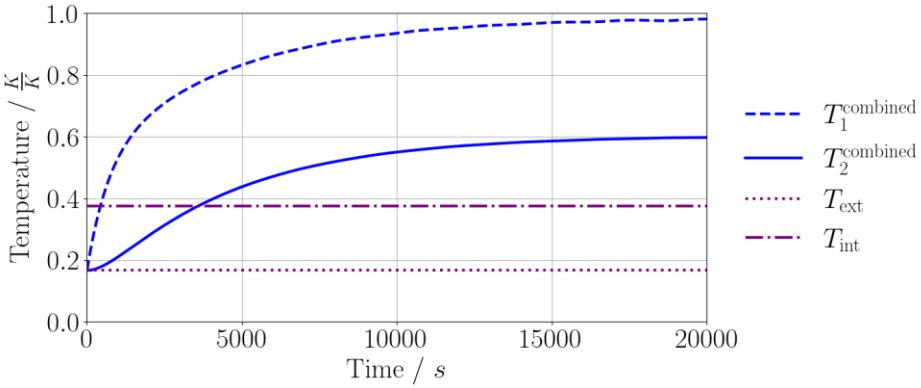

Figure 9: Resulting transient curves based on the heat capacity information from the experimental data and the stationary information from CFD-Simulation.

6 Conclusion

This paper achieved the calculation of a transient response for a stationary CFD simulation based on transient experimental measurements. The results were achieved for the component space of the IPBasis by leveraging a lumped parameter thermal network approach. The global parameter fitting of the experimental data represents a novel extension to the state-of-the-art minimization algorithm for estimating LPTN parameters from temperature data, achieving a RMSE of 0.91K. This work demonstrated the extraction of LPTN parameters from a CFD simulation. The assembly of the transient curve from the stationary data and the heat capacity information was demonstrated in section 5.1 as a proof of concept with 100% accuracy.

It is anticipated that utilizing multiple experimental files simultaneously will enhance the global fitting approach, allowing for more accurate determination of heat capacities. However, this assumption requires further investigation, and establishing a guideline for the optimal number of files necessary in an n-body LPTN would be advantageous. Additionally, the fitting of parameters derived from the CFD simulation is based on the stationary temperature point, specifically the highest temperature observed. Consequently, when fitting temperature-dependent parameters, such as the convection heat transfer coefficient, the estimated values are too high in the transient phases calculated. This tendency leads to an underestimation of temperatures, as too much energy is dissipated. To address this issue, introducing nonlinearity into the system could provide a viable solution. Future work should focus on developing and testing this approach using a transient CFD model.

7 Reference list

[AhRF22] Saad Ahmed, Hermann Rottengruber, Markus Full. Hybrid model for exhaust systems in vehicle thermal management simulations. In: *Automotive and Engine Technology* Bd. 7 (2022), Nr. 1–2, S. 115–136

[Bmwa25] BMW AG. *Das Energie- und umwelttechnische Versuchszentrum der BMW Group*. URL https://www.press.bmwgroup.com/deutschland/article/detail/T0080599DE/das-energie-und-umwelttechnische-versuchszentrum-der-bmw-group?language=de

[DhKA23] Amol R. Dhumal, Atul P. Kulkarni, Nitin H. Ambhore. A comprehensive review on thermal management of electronic devices. In: *Journal of Engineering and Applied Science* Bd. 70 (2023), Nr. 1, S. 140

[Disc16] Mario Disch. *Numerische und experimentelle Analyse von instationären Lastfällen im Rahmen der thermischen Absicherung im Gesamtfahrzeug*. Wiesbaden : Springer Fachmedien Wiesbaden, 2016

[Elle17] Jan Eller. *Stützpunktbasierter Ansatz zur Vorhersage von Bauteiltemperaturkollektiven im Thermomanagement des Gesamtfahrzeugs*. Wiesbaden : Springer Fachmedien Wiesbaden, 2017

[Enri15] Joshua Enriquez-Geppert. *Numerische und experimentelle Analyse der Wärmeübertragung einer Abgasanlage im Gesamtfahrzeug*. Stuttgart, University of Stuttgart, 2015

[FrER23] Lukas Freytag, Wolfram Enke, Hermann Rottengruber. Leveraging Historical Thermal Wind Tunnel Data for ML-Based Predictions of Component Temperatures for a New Vehicle Project. In: *SAE Technical Paper*. 2023-01-1216, 2023

[FrRE24] Lukas Freytag, Hermann Rottengruber, Wolfram Enke. Monitoring the Thermal Aging of Rubber Bearings Using Virtual Temperature Sensors. In: *SAE Technical Paper*. 2024-01-5099, 2024

[Gheb13] Daniel Ghebru. *Modellierung und Analyse des instationären thermischen Verhaltens von Verbrennungsmotor und Gesamtfahrzeug*. Berlin, Karlsruher Institut für Technologie (KIT), 2013

[KeRE25] Maximilian Kehe, Hermann Rottengruber, Wolfram Enke. Lumped Parameter Thermal Network (LPTN) for Automotive Components: Modeling, Simulation, System Identification, and Parameter Estimation. In: *SAE Technical Paper*. 25NETP-0072, 2025 (in review)

[MeRT91] P.H. Mellor, D. Roberts, D.R. Turner. Lumped parameter thermal model for electrical machines of TEFC design. In: *IEE Proceedings B Electric Power Applications* Bd. 138 (1991), Nr. 5, S. 205